AMERICAN SCIENTIFIC PUBLISHERS

Journal of Nanofluids
Vol. 8, pp. 1273–1280, 2019
(www.aspbs.com/jon)

Steady Electrical MHD Mixed Convection Flow of Nanofluid Under the Influence of Exponentially Decreasing Freestream Velocity with the Effect of Heat Generation/Absorption

G. Revathi[1], M. Revathy[2,*], M. Marudai[1], and S. Jayanthi[3]

[1]*Department of Mathematics, Bharathidasan University, 620024, Tamilnadu, India*
[2]*Alliance College of Engineering and Design, Bangalore 562106, India*
[3]*BMS College of Engineering, Bangalore 560019, India*

The present analysis is about the simultaneous effect of magnetic energy, electrical conductivity and heat generation/absorption of a steady laminar incompressible nanofluid under the influence of exponentially decreasing free stream velocity. Using the non-similarity transformation the coupled nonlinear partial differential equations governing the flow are made dimensionless. Non-linear differential equations are solved by implicit finite difference scheme in combination with quasilinearization technique. The effect of factors such as Brownian motion parameter, thermophoresis parameter, Lewis number, buoyancy parameter, magnetic parameter, heat generation or absorption parameter are investigated on the dimensionless velocity, temperature and nanoparticle concentration profiles and their respective gradients. It is found that, the presence of electrical field, magnetic field and nano particle concentration have prominent effects on fluid flow and heat transfer characteristics.

KEYWORDS: Nanofluid, Incompressible, Non-Similar Solution, Exponentially Decreasing Free Stream Velocity.

1. INTRODUCTION

Nanofluids are engineered by suspending nanoparticles of sizes below 10 nm, in the base fluid like water, oil, lubricants and ethylene glycol which enhances the properties of the fluid, is of much interests for many researchers. *In 1995*[1] *has conceived the concept of nanofluids, from then scientists and engineers have made scientific breakthrough in discovering thermal properties of nanofluid and developing unconventional models of nanofluid and identifying opportunities to develop the next generation coolants for computers, nuclear reactors, microelectronic equipments*. Other benefits envisioned for nanofluid include decreased demand for pumping power, reduced inventory of heat transfer fluid and significant energy savings. *In 2006*[2] *has made a comprehensive survey on convective transport in nanofluids.* Many investigations have been made about heat transfer enhancement in nanofluid.[3–5]

Electrically conducting fluid in the presence of magnetic field draws much attention of many researchers for its application includes surface coating of metals, crystal growth and reactor cooling.[6] The present study is about the flow and heat transfer in an electrically conducting fluid adjacent to the surface. The interaction of the magnetic field and the moving electric charge carried by the flowing fluid induces a force which tends to oppose the fluid motion. The velocity near the leading edge is small, so the magnetic force which is proportional to the magnitude of the longitudinal velocity and acts in the opposite direction is also very small. The influence of the magnetic field on the boundary layer is exerted only through induced forces within the boundary layer with no additional effects arising from the free stream pressure gradient. Magneto-hydrodynamic application in fusion power is the creation and containment of hot plasmas by electro magnetic forces, since material walls would be destroyed. *The effect of heat transfer in a MHD boundary layer flow over a continuous moving wavy surface is investigated by* Ref. [7]. *There are several investigations in literature on MHD mixed convection flow over different geometries are given in* Refs. [8–12]. The effect of mhd with mixed convection flow over an inclined cylinder for nanofluids is analyzed in Ref. [13].

In the work of Ref. [14] a study is done to analyze the effect of magneto-hydrodynamic in flow of exponentially decreasing free stream velocity in the region of

*Author to whom correspondence should be addressed.
Email: revathy.m@alliance.edu.in
Received: 9 September 2018
Accepted: 1 November 2018

ARTICLE

separation. In the work of Ref. [15], the simultaneous effects of mixed convection, heat and mass transfer and heat generation/absorption are studied for the boundary layer flow. In the work of Ref. [16], how nanoparticles affect the separation region of the forced convective boundary layer flow is reported. As a step forward to the eventual development of the above literature the present study is considered to analyze the effect of electrically conducting magneto-hydrodynamic fluid flow with exponentially decreasing free stream velocity in the presence of heat generation/absorption. Author is motivated to the present study, due to its useful applications in cooling electronic equipment, Cooling turbine blades, combustion chambers, chemical processes, cooling of nuclear reactors, wide angle diffuser, high performance heat exchangers, energy systems equipment and flow in valves. *Also it has specific application in geothermal reservoirs, thermal insulation, cooling of nuclear reactors and enhanced oil recovery. Present results are compared with the results of* Ref. [17] *and are in good agreement.*

2. MATHEMATICAL FORMULATION

Consider a two-dimensional steady electrical MHD mixed convection flow of nanofluid having exponentially decreasing free stream velocity in the presence of heat generation/absorption. Let x and y be the curvilinear coordinates along and perpendicular to the body surface, respectively and let u and v be the corresponding velocity components (see Fig. 1). The geometry is placed in a flow field with the free stream velocity u_∞ is taken as constant. L is the characteristic length. The surface is maintained with prescribed wall temperature T_w different from the temperature at free stream T_∞. *When* $(T_w > T_\infty)$ *the flow corresponds to assisting flow and when* $(T_w < T_\infty)$ *the flow corresponds to opposing flow*. Similarly, the value of the nanoparticle volume fraction at the surface C_w is different from the nanoparticle concentration at free stream C_∞ $(C_w > C_\infty)$. Uniform magnetic field of strength B_0 which is applied in y-direction and the gravitational acceleration g acts downwards parallel to the x-direction and σ is the electrical conductivity (assumed to be constant). Under these assumptions, the equations of conservation of mass, momentum, energy and nanoparticle concentration governing the mixed convective boundary layer flow is given below.[18,19]

$$u_x + v_y = 0 \tag{1}$$

$$uu_x + vu_y = u_e(u_e)_x + \nu u_{yy} + \frac{\sigma B_0^2}{\rho_f}(u_e - u) + g\beta_t(T - T_\infty) + g\beta_c(C - C_\infty) + \frac{\sigma E_0 B_0}{\rho_f} \tag{2}$$

$$uT_x + vT_y = \frac{\kappa_f}{(\rho C_P)_f}T_{yy} + \frac{(\rho C_P)_p}{(\rho C_P)_f}\left[D_B C_y T_y + \frac{D_T}{T_\infty}T_y^2\right] + \frac{Q_0}{(\rho C_P)_f}(T - T_\infty) \tag{3}$$

$$uC_x + vC_y = D_B C_{yy} + \frac{D_T}{T_\infty}T_{yy} \tag{4}$$

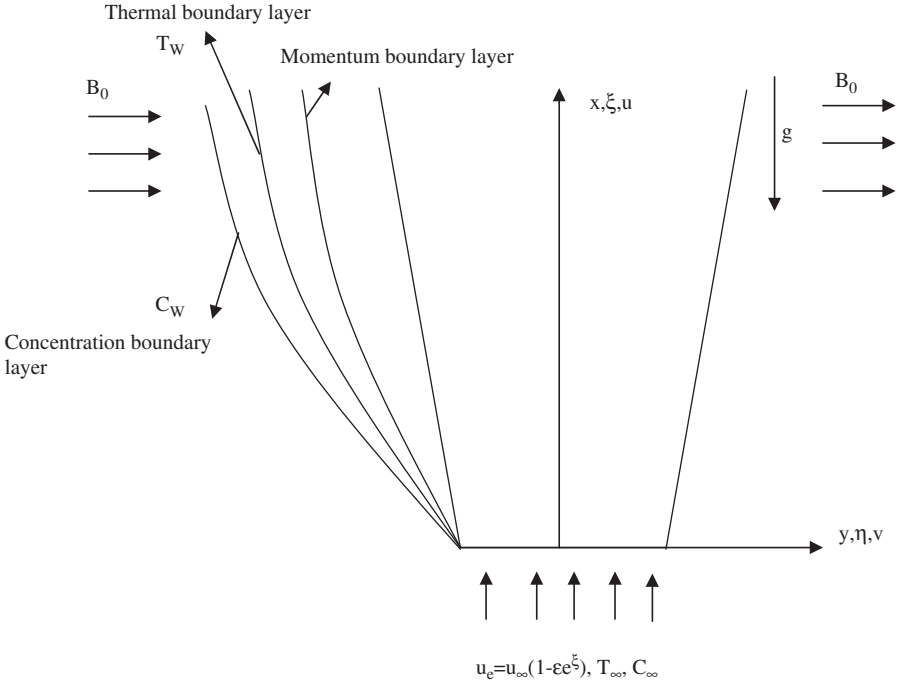

Fig. 1. Flow geometry.

Boundary conditions are

$$u(x,0)=0, \quad v(x,0)=0, \quad T(x,0)=T_w, \quad C(x,0)=C_w \tag{5}$$

$$u(x,\infty)=u_e(x), \quad T(x,\infty)=T_\infty, \quad C(x,\infty)=C_\infty \tag{6}$$

where $\alpha=\kappa/(\rho C_P)_f$ is the thermal diffusivity of the base fluid, $\tau=(\rho C_P)_p/(\rho C_P)_f$ is the ratio of the nanoparticle heat capacity and the base fluid heat capacity. $(\rho C_P)_f$ and $(\rho C_P)_p$ are the specific heat parameters of the base fluid and nanoparticle, respectively. D_B is the Brownian diffusion coefficient and D_T is the thermophoresis diffusion coefficient. E_0 is the electrical field factor. The above dimensional governing equations with the initial and boundary conditions are made non-dimensional using non-similarity transformations given below,

$$\Psi(x,y)=\sqrt{u_e\nu x}f(\xi,\eta), \quad \xi=\frac{x}{L}, \quad \eta=\sqrt{\frac{u_e}{\nu x}}y$$

$$u=\frac{\partial\Psi}{\partial y}, \quad v=-\frac{\partial\Psi}{\partial x}, \quad G=\frac{T-T_\infty}{T_w-T_\infty}$$

$$N=\frac{C-C_\infty}{C_w-C_\infty}, \quad Re=\frac{u_\infty L\rho}{\mu_\infty},$$

$$u_e=u_\infty(1-\epsilon\exp\xi) \quad 0<\epsilon<1$$

Now Eqs. (1)–(4) with initial and boundary conditions (5)–(6) becomes,

$$F_{\eta\eta}+m(1-F^2)+\left(\frac{1+m}{2}\right)fF_\eta+MP(\xi)(1-F)+\lambda S(\xi)(G+QN)+MS(\xi)E=\xi(FF_\xi-f_\xi F_\eta) \tag{7}$$

$$\frac{1}{Pr}G_{\eta\eta}+(Nb)N_\eta G_\eta+(Nt)G_\eta^2+\left(\frac{1+m}{2}\right)fG_\eta+DP(\xi)G=\xi(FG_\xi-G_\eta f_\xi) \tag{8}$$

$$\frac{1}{Le}\left(N_{\eta\eta}+\frac{Nt}{Nb}G_{\eta\eta}\right)+\left(\frac{1+m}{2}\right)fN_\eta=\xi(FN_\xi-N_\eta f_\xi) \tag{9}$$

$$F(\xi,0)=0, \quad G(\xi,0)=1, \quad N(\xi,0)=1 \tag{10}$$

$$F(\xi,\infty)=1, \quad G(\xi,\infty)=0, \quad N(\xi,\infty)=0 \tag{11}$$

where $m=x/u_e du_e/dx$, MHD parameter $M=\sigma B_0^2 L/(\rho_f u_\infty)$, $P(\xi)=\xi(u_\infty/u_e)$, $S(\xi)=\xi(u_\infty/u_e)^2$, mixed convection parameter $\lambda=Gr_L/Re_L^2$, $Q=\lambda^*/\lambda$, source term $D=Q_0L/((\rho C_P)_f u_\infty)$, $Nb=\tau D_B(C_w-C_\infty)/\nu_f$ is the Brownian motion number, $Nt=\tau D_T(T_w-T_\infty)/\nu_f T_\infty$ is the thermophoresis number and $Le=\nu_f/D_B$ is the Lewis number. *It is important to note that $\lambda>0(T_w>T_\infty)$ corresponds to assisting flow, $\lambda<0(T_w<T_\infty)$ corresponds to opposing flow, $\lambda=0(T_w=T_\infty)$ corresponds to forced convection case. The parameter Q is zero for no buoyancy effect due to mass diffusion, Q is infinite for no buoyancy effect due to thermal diffusion, Q is unity for thermal and mass buoyancy forces of the same strength, Q is positive for the combined buoyancy forces which are driving the flow and negative for the buoyancy forces which are opposing each other. The present study is for the flow driven by the combined buoyancy forces due to mass diffusion and thermal diffusion, and the parameter Q is considered as $Q=0.1$.*

3. METHOD OF SOLUTION

Equations (7)–(9) are coupled non-linear partial differential equations and those are linearized by using quasi linearization technique.[20,21] This technique is an application of the Newton Raphson Kantrovich approximation method in function space by Ref. [20]. Applying quasilinearization technique we get a linear system of equations.

$$X_1^iF_{\eta\eta}^{i+1}+X_2^iF_\eta^{i+1}+X_3^iF_\xi^{i+1}+X_4^iF^{i+1}+X_5^iG^{i+1}+X_6^iN^{i+1}=X_7^i \tag{12}$$

$$Y_1^iG_{\eta\eta}^{i+1}+Y_2^iG_\eta^{i+1}+Y_3^iG_\xi^{i+1}+Y_4^iG^{i+1}+Y_5^iF^{i+1}+Y_6^iN_\eta^{i+1}=Y_7^i \tag{13}$$

$$Z_1^iN_{\eta\eta}^{i+1}+Z_2^iN_\eta^{i+1}+Z_3^iN_\xi^{i+1}+Z_4^iF^{i+1}+Z_5^iG_\eta^{i+1}+Z_6^iG_\xi^{i+1}+Z_7^iG^{i+1}=Z_8^i \tag{14}$$

The boundary conditions become

$$F^{i+1}(\xi,0)=0, \quad G^{i+1}(\xi,0)=1, \quad N^{i+1}(\xi,0)=1 \tag{15}$$

$$F^{i+1}(\xi,\infty)=1, \quad G^{i+1}(\xi,\infty)=0, \quad N^{i+1}(\xi,\infty)=0 \tag{16}$$

Here the iterative indices are dropped from the dependent variable and the coefficients X_k, Y_k and Z_k, $k=1,2,3,\ldots,8$ are known functions as they contain only ith iteration values and are given below

$$X_1^i=1, \quad X_2^i=\xi f_\xi+\left(\frac{1+m}{2}\right)f, \quad X_3^i=-\xi F$$

$$X_4^i=-(\xi F_\xi+2mF+MP(\xi)),$$

$$X_5^i=\lambda S(\xi), \quad X_6^i=\lambda S(\xi)Q$$

$$X_7^i=-[m(1+F^2)+\xi F_\xi F+MS(\xi)E+MP(\xi)],$$

$$Y_1^i=1/Pr, \quad Y_2^i=\xi f_\xi+NbN_\eta+2NtG_\eta+\left(\frac{1+m}{2}\right)f,$$

$$Y_3^i=-\xi F, \quad Y_4^i=DP(\xi), \quad Y_5^i=-\xi G_\xi, \quad Y_6^i=NbG_\eta,$$

$$Y_7^i=NtG_\eta^2-\xi FG_\xi+NbG_\eta N_\eta$$

$$Z_1^i=1, \quad Z_2^i=Le\left(\frac{1+m}{2}\right)f-CNNbG_\eta+Le\xi N_\xi,$$

ARTICLE

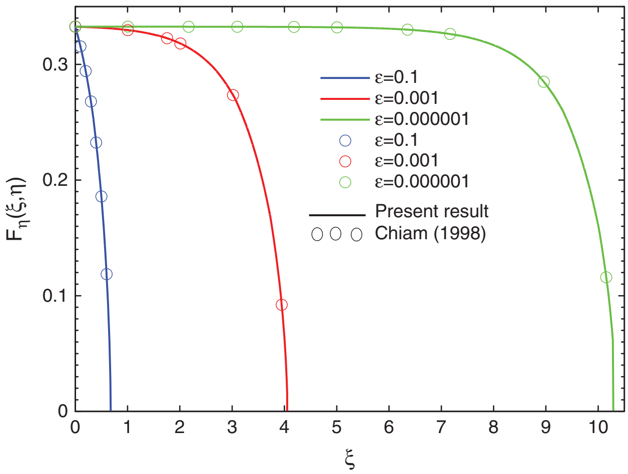

Fig. 2. Comparison figure with the results of Chaim (1998) $Le = Nb = Nt = E = D = M = 0$.

$$Z_3^i = -Le\xi F \quad Z_4^i = CN\xi G_\xi - Le\xi N_\xi,$$

$$Z_5^i = -NtPr\left[\frac{\xi f_\xi}{Nb} + N_\eta + 2\frac{Nt}{Nb}G_\eta + \frac{1}{Nb}\left(\frac{1+m}{2}\right)f\right]$$

$$Z_6^i = CN\xi F, \quad Z_7^i = -CNDP(\xi)$$

$$Z_8^i = CN\xi FG_\xi - CNNtG_\eta^2 - CNNbG_\eta N_\eta - Le\xi FN_\xi$$

where $CN = (Nt/Nb)Pr$. In Ref. [22] the detailed explanation about the method for partial differential equations is given. Now the derivatives are discretized using central difference scheme for η direction and backward difference scheme for ξ direction along with the initial and boundary conditions in order to get the equations in difference form. Finally, at each iteration step, the equation reduces to a system of algebraic equations in block tri-diagonal form which is solved using varga algorithm.[23] The step size in the η-direction is taken as $\Delta\eta = 0.01$ throughout the computation. A further decrease in $\Delta\eta$ does not change the results up to the fourth decimal place. The step size $\Delta\eta$ and the position of the edge of the boundary layer η_∞ are to be regulated for different value of the parameters to sustain the accuracy. In the present work the value of η_∞ is taken as 6. The step size in the ξ-direction, for small values of ξ has been chosen as $\Delta\xi = 0.01$ and then it is being decreased to $\Delta\xi = 0.001$. The step size is reduced further to $\Delta\xi = 0.0001$ near the neighborhood of the zero skin friction. This has been done because, the convergence becomes slower around the point of vanishing skin friction. The present work is to analyze the effects of Brownian motion parameter, thermophoresis parameter and Lewis number through numerical solutions.

4. RESULTS AND DISCUSSION

The present results are compared with the already existing literature results.[17] Comparison shows excellent agreement and some of the comparisons of $F_\eta(\xi, 0)$ for $Nt = Le = D = E = M = Nb = 0$ with deceleration parameters $\epsilon = 0.1$, $\epsilon = 0.001$ and $\epsilon = 0.000001$ are displayed in Figure 2. Figure 3 depicts flow field of dimensionless velocity, temperature and nanoparticle concentration profiles and it is found that as magnetic parameter increases the velocity, temperature and nanoparticle concentration distribution decreases at a particular point in the flow region. This is because there would be a decreasing

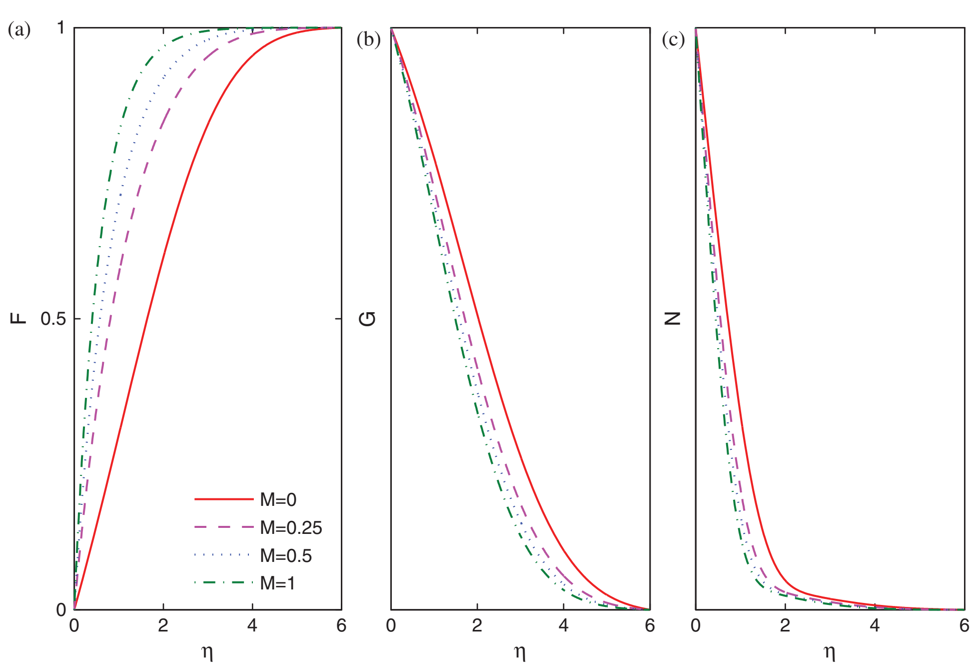

Fig. 3. Velocity, temperature and nanoparticle concentration profiles for various magnetic parameter (M) at $\xi = 1.5$, for the values of $Nb = Nt = 0.45$, $Le = 10$, $Pr = 0.72$, $\epsilon = 0.001$, $Q = 0.1$, $E = 0$, $D = 0$, $\lambda = 0.1$.

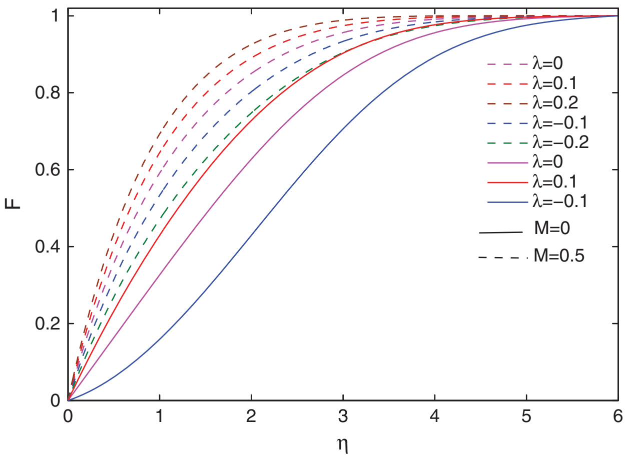

Fig. 4. Velocity profile for various mixed convection parameter or buoyancy parameter (λ) at the values of $Nt = Nb = 0.45$, $Le = 10$, $Pr = 0.72$, $\epsilon = 0.001$, $Q = 0.1$, $E = 0$, $D = 0$.

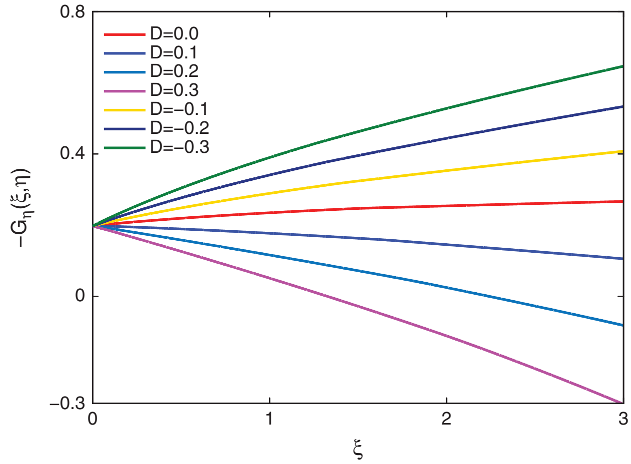

Fig. 6. Temperature gradient as a function of heat generation or source ($D > 0$)/heat absorption or sink ($D < 0$) at the values of $Nt = Nb = 0.45$, $Le = 10$, $Pr = 0.72$, $\epsilon = 0.001$, $Q = 0.1$, $E = 0$, $M = 0$.

of the velocity, temperature and nanoparticle concentration boundary layer thickness with the increasing magnetic parameter.

Effect of mixed convection parameter on velocity profile is depicted in Figure 4. As the increasing value of mixed convection parameter (λ), the velocity boundary layer thickness is decreasing. It is significant to note that the buoyancy opposing force ($\lambda < 0$) reduces the magnitude of the velocity significantly within the momentum boundary layer for both the values of magnetic parameters $M = 0$ and $M = 0.5$. Buoyancy parameter is the ratio of the buoyancy to the viscous force which will accelerate the fluid and works as a pressure gradient. In Figure 5 the effect of electrical parameter (E) is depicted. As the electrical parameter increases the velocity and the temperature boundary layer thickness decrease at a particular point of the flow region. It is found that for the larger values of electrical parameter, lower heat transfer effect is produced.

The effect of heat generation or absorption parameter ($D > 0$ or $D < 0$) on the temperature gradient is plotted in Figure 6. It is noticed that the temperature gradient decrease with heat generation but it increase with heat absorption. This is because of the thermal state of the fluid increase due to heat generation and it causes temperature

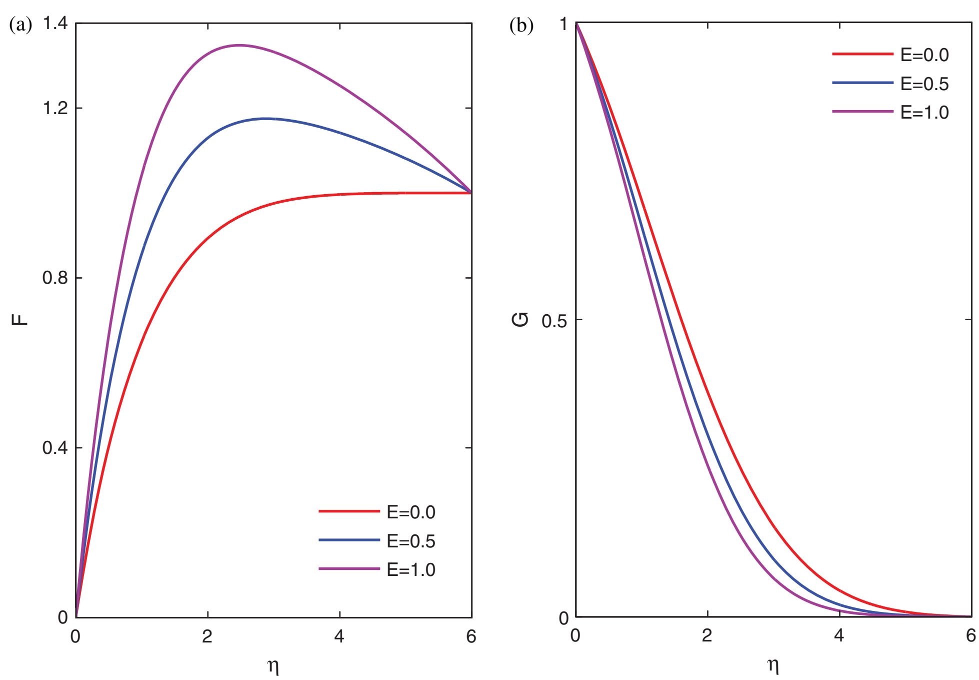

Fig. 5. Velocity and temperature profiles for various electrical parameter (E) at the values of $Nt = Nb = 0.45$, $Le = 10$, $Pr = 0.72$, $\epsilon = 0.001$, $Q = 0.1$, $\lambda = 0$, $D = 0$.

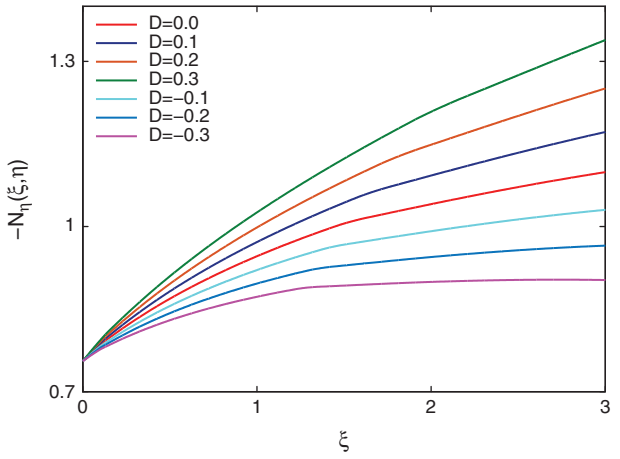

Fig. 7. Nanoparticle concentration gradient as a function of heat generation or source ($D > 0$)/heat absorption or sink ($D < 0$) at the values of $Nt = Nb = 0.45$, $Le = 10$, $Pr = 0.72$, $\epsilon = 0.001$, $Q = 0.1$, $E = 0$, $M = 0$.

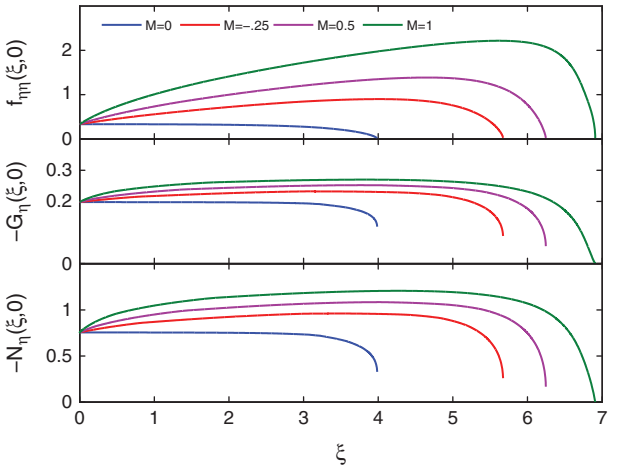

Fig. 9. Velocity, temperature and nanoparticle concentration gradients as a function of MHD parameter (M) at the values of $Nt = Nb = 0.45$, $Le = 10$, $Pr = 0.72$, $\epsilon = 0.001$, $Q = 0.1$, $\lambda = 0$, $E = 0$, $D = 0$.

and thermal boundary layer to increase and consequently results in the negative temperature gradient and hence the heat transfer rate decreases with heat generation ($D > 0$). The large heat generation parameter causes the negative temperature gradient value. From Figure 7, it is found that the nanoparticle concentration gradient increase as the increase in heat generation parameter. The increase in the fluid temperature causes decrease in the nanoparticle concentration boundary layer thickness that results in increase of the nanoparticle concentration gradient.

In Figure 8, the effect of electrical parameter (E) is studied on velocity, temperature and nanoparticle concentration gradients. It is found that as the electrical parameter increases the velocity, temperature and nanoparticle concentration gradient increase. The reason is that as electrical parameter increases, the thickness of velocity, temperature and nanoparticle concentration boundary layer decrease hence the gradient value increases. It is found from Figure 9 that as MHD parameter increase, the velocity, temperature and nanoparticle concentration gradients also increases and attain maximum value at some point, then starts to decrease. Here the velocity gradient reaches zero gradient value (separation point) while temperature and nanoparticle concentration gradients breaks away before it reach zero gradient value. Hence MHD parameter helps to delay separation. In particular for $M = 1$, it is observed that the point of separation delays 42.3% as the MHD parameter increases from $M = 0$ to $M = 1$.

Figure 10 represent the effect of mixed convection parameter or buoyancy parameter (λ) on velocity, temperature and nanoparticle concentration gradients. It is found that as the buoyancy parameter increase the

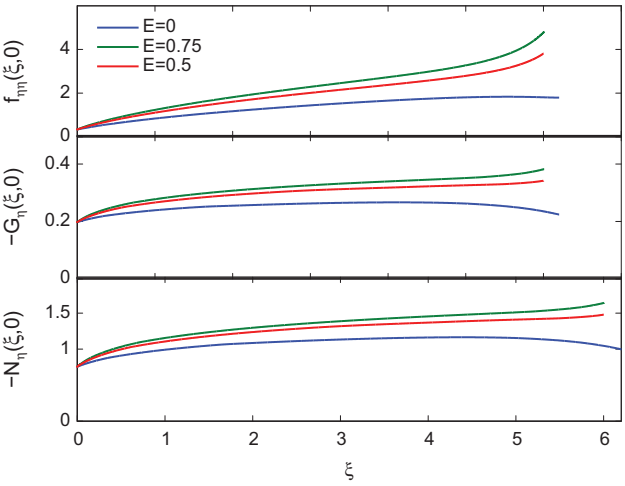

Fig. 8. Velocity, temperature and nanoparticle concentration gradients as a function of electrical parameter (E) at the values of $Nt = Nb = 0.45$, $Le = 10$, $Pr = 0.72$, $\epsilon = 0.001$, $Q = 0.1$, $\lambda = 0$, $D = 0$, $M = 0$.

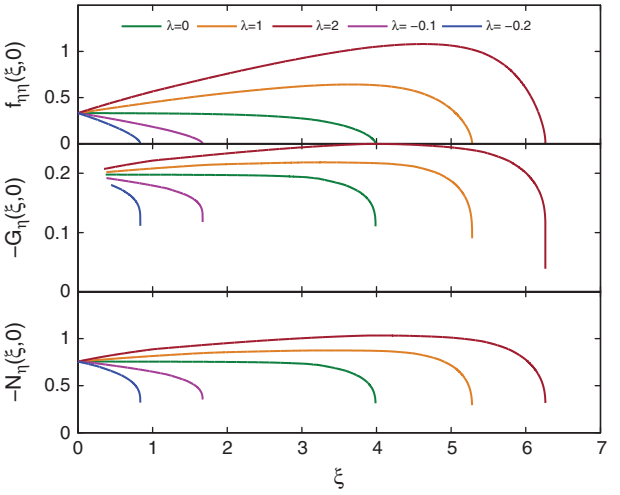

Fig. 10. Velocity, temperature and nanoparticle concentration gradients as a function of mixed convection parameter at the values of $Nt = Nb = 0.45$, $Le = 10$, $Pr = 0.72$, $\epsilon = 0.001$, $Q = 0.1$, $D = 0$, $M = 0$.

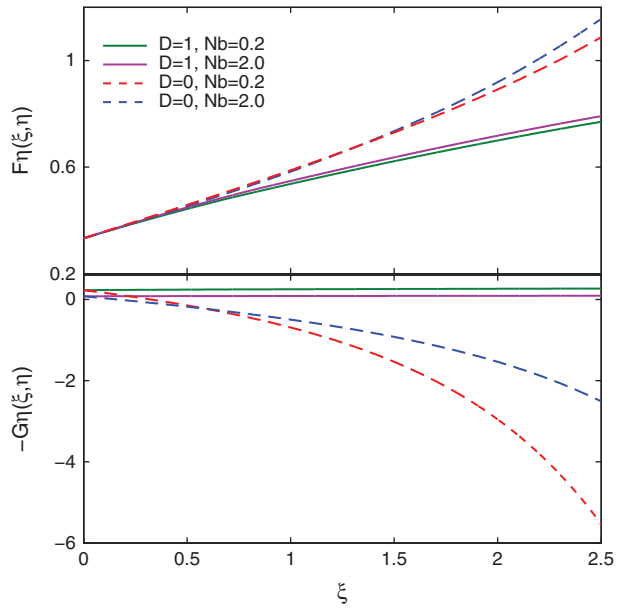

Fig. 11. Velocity and temperature gradients as a function of Brownian motion parameter (Nb) at the values of $Nt = 0.45$, $Le = 10$, $Pr = 0.72$, $\epsilon = 0.001$, $Q = 0.1$, $M = 0$, $\lambda = 0$.

velocity gradient increases and attain maximum value then decreases to reach zero gradient value (separation point). It is significant here to note that the buoyancy parameter delays separation. In particular for $\lambda = 2$, it is observed that the point of separation delays 36.34% as the buoyancy parameter increases from $\lambda = 0$ to $\lambda = 2$. Similarly as buoyancy parameter increases the temperature and nanoparticle concentration gradients also increase then at some point start to decrease and breaks away before it

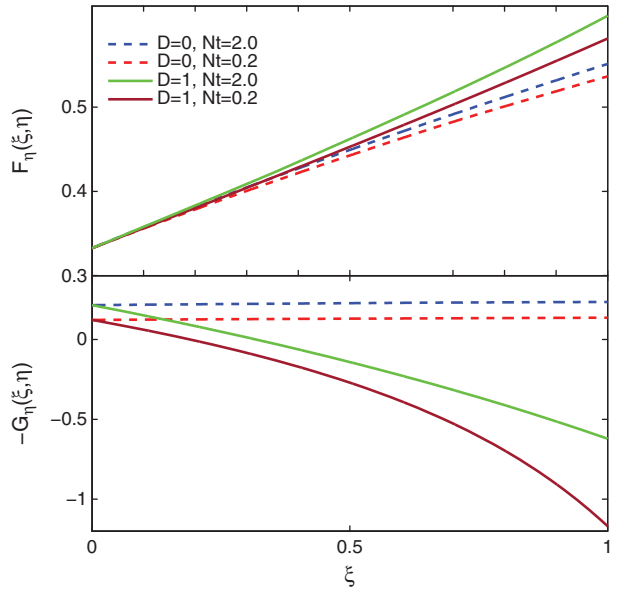

Fig. 12. Velocity and temperature gradients as a function of thermophoresis parameter (Nt) at the values of $Nb = 0.45$, $Le = 10$, $Pr = 0.72$, $\epsilon = 0.001$, $Q = 0.1$, $M = 0$, $\lambda = 0$.

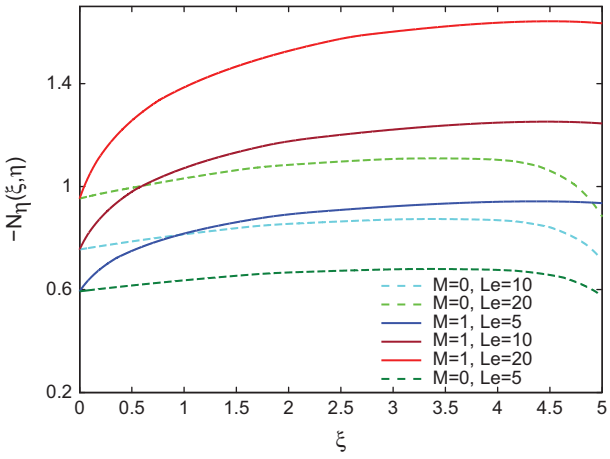

Fig. 13. Nanoparticle concentration gradient as a function of Lewis number (Le) at the values of $Nb = Nt = 0.45$, $Pr = 0.72$, $\epsilon = 0.001$, $Q = 0.1$, $\lambda = 0$.

reaches zero gradient value. *The effect of both Brownian motion and thermophoresis parameters on nanoparticle concentration gradient is less compared to the velocity and temperature gradients which could be seen in* Figures 11 and 12 *respectively.* As Brownian motion and thermophoresis parameters increase the velocity gradient and temperature gradient increase. The effects of Brownian motion and thermophoresis parameter with heat generation $(D = 1)$ gives negative temperature gradient. Figure 13 explains the effect of Lewis number on nanoparticle concentration gradient. It is observed that as Lewis number with buoyancy parameter increases nanoparticle concentration gradient also increases.

5. CONCLUSIONS

Non-similar solutions have been obtained from the starting point of the stream-wise co-ordinate to the point of separation. Magnetic and buoyancy parameters have same effects on the transport phenomina of the boundary layer flow, that is both parameters delay separation when they increase. Velocity, temperature and nanoparticle concentration gradients increase as electrical parameter increases. There is an overshoot in the velocity profile for higher value of electrical parameter $(E = 1)$. Heat generation causes decrease in temperature gradient while heat absorption causes increase in temperature gradient. Heat generation causes increase in nanoparticle concentration gradient while heat absorption causes decrease in nanoparticle concentration gradient. Increasing magnetic parameter causes decrease in flow velocity, temperature and nanoparticle concentration but increases velocity, temperature and nanoparticle concentration gradients. The nanofluid flow temperature is decreased due to the increase in electrical parameter also it causes increase in temperature gradient. As Brownian motion and thermophoresis parameters increase the velocity and temperature gradients

increase. Nanoparticle concentration gradient increases with Lewis number.

LIST OF ABBREVIATIONS

B_0 Magnetic induction
C_f Skin friction coefficient
c_p Specific heat at constant pressure ($kJ \cdot kg^{-1} \cdot K^{-1}$)
D Heat generation or absorption parameter
D_B Brownian diffusion coefficient
D_T Thermophoresis diffusion coefficient
E Electrical parameter
E_0 Electrical field factor
f Dimensionless stream function
F Dimensionless velocity component in the x-direction
g Acceleration due to gravity
G Dimensionless temperature
Gr_L, Gr_L^* Grashf numbers due to temperature and concentration respectively.
L Characteristic length
Le Lewis number
M MHD parameter
m Pressure gradient parameter
N Dimensionless concentration
Nb Brownian motion parameter
Nt Thermophoresis parameter
Pr Prandtl number
Q Ratio of the buoyancy forces or ratio of Grashof numbers
Q_0 Heat generation coefficient
Re_L Reynolds number
T Temperature (K)
u, v Dimensional velocity components in x and y directions respectively ($m \cdot s^{-1}$).

Greek Symbols

α Thermal diffusivity of the base fluid
β Pressure gradient
β_t, β_c Volumetric coefficients of thermal and concentration expansions respectively.
η, ξ Transformed coordinates
κ Thermal conductivity ($W \cdot m^{-1} \cdot K^{-1}$)
λ Mixed convection parameter
μ Dynamic viscosity ($kg \cdot m^{-1} \cdot s^{-1}$)
ν_f Kinematic viscosity of fluid
ρ Density ($kg \cdot m^{-3}$)
$(\rho C_P)_f$, $(\rho C_P)_P$ Heat capacity of the fluid and nanoparticle respectively
σ Electrical conductivity
τ Ratio of nanoparticle heat capacity and base fluid heat capacity.
ψ Dimensional stream function ($m^2\ s^{-1}$)
$\Delta\eta$, $\Delta\xi$ Step sizes in η and ξ directions respectively.

Subscripts

∞ Conditions in the free stream
e, w Conditions at the edge of the boundary layer and on the surface, respectively
ξ, η Partial derivatives with respect to these variables.

Compliance with Ethical Standards

The first author has received the grant from the University Grant Commission of India under the scheme of Dr. Kothari postdoctoral research fellowship (Grant Number: F.4-2/2006(BSR)/MA/14-15/0010).

Acknowledgments: The authors are grateful to referees for their excellent comments which helped us to improve the manuscript.

References and Notes

1. S. U. S. Choi, *ASME-Publications-Fed* 231, 99 **(1995)**.
2. J. Buongiorno, *J. Heat Transfer* 128, 240 **(2006)**.
3. K. Das, P. R. Duari, and P. K. Kundu, *Alexandria Engineering Journal* 53, 737 **(2014)**.
4. X. Q. Wang and A. S. Mujumdar, *Brazilian Journal of Chemical Engineering* 25, 613 **(2008)**.
5. S. Kakac and A. Pramuanjaroenkij, *Int. J. Heat Mass Transfer* 52, 3187 **(2009)**.
6. T.Hayat, S. Shehzad, and A. Alsaedi, *Applied Mathematics and Mechanics* 33, 1301 **(2012)**.
7. M. A. Hossain and I. Pop, *Archives of Mechanics* 48, 813 **(1996)**.
8. A. J. Chamkha and A. M. Aly, *Chem. Eng. Commun.* 198, 425 **(2010)**.
9. L. Pslaru-Dnescu, A. M. Morega, G. Telipan, M. Morega, J. B. Dumitru, and V. Marinescu, *IEEE Transactions on Magnetics* 49, 5489 **(2013)**.
10. F. Selimefendigil and H. F. Oztop, *Journal of the Taiwan Institute of Chemical Engineers* 45, 2150 **(2014)**.
11. K.-L. Hsiao, *Appl. Therm. Eng.* 98, 850 **(2016)**.
12. F. Selimefendigil and H. F. Oztop, *Int. J. Heat Mass Transfer* 78, 741 **(2014)**.
13. R. Dhanai, P. Rana, and L. Kumar, *Powder Technol.* 288, 140 **(2016)**.
14. M. Alim, M. Rahman, and M. Karim, *Journal of Naval Architecture and Marine Engineering* 5, 11 **(2008)**.
15. P. M. Patil, H. S. Ramane, S. Roy, V. Hindasageri, and E. Momoniat, *Int. J. Heat Mass Transfer* 104, 392 **(2017)**.
16. G. Revathi and M. Marudai, *J. Nanofluids* 6, 777 **(2017)**.
17. T. Chiam, *Acta Mechanica* 129, 255 **(1998)**.
18. W. A Khan and I. Pop, *Int. J. Heat Mass Transfer* 53, 2477 **(2010)**.
19. M. Mustafa, T. Hayat, I. Pop, S. Asghar, and S. Obaidat, *Int. J. Heat Mass Transfer* 54, 5588 **(2011)**.
20. R. E. Bellman and R. E. Kalaba, *Quasilinearization and Nonlinear Boundary-Value Problems* 121, 280 **(1965)**.
21. K. Inouye and A. Tate, *AIAA Journal* 12, 558 **(1974)**.
22. P. J. Singh and S. Roy, *Int. J. Heat Mass Transfer* 50, 949 **(2007)**.
23. R. S. Varga, Matrix iterative analysis, Springer Series in Computational Mathematics, Second edition, New York **(2009)**.